J Nanostruct 15(2): 771-787, Spring 2025

RESEARCH PAPER

Enhanced Wound Repair in Rats via a Chitosan-Based Transdermal Patch with Selenium Nanoparticles and Platelet-Rich Plasma

Mohammad Amin Kaboli [1], ***Alaa A. Hashim*** [2,3], ***Dhiya Altememy*** [4], ***Elham Moghtadaei-Khorasgani*** [5], ***Abdulhamid Alikhani*** [6], ***Amir Mohamad Jannesari*** [7], ***Narges Najafi*** [8], ***Moosa Javdani*** [9]**, ***Pegah Khosravian*** [10]*

[1] *Department of Tissue Engineering and Applied Cell Sciences, School of Advanced Technologies in Medicine, Shahid Beheshti University of Medical Sciences, Tehran, Iran*

[2] *Department of Pharmaceutics, College of Pharmacy, Ahl AL-Bayt University, Karbala, Iraq*

[3] *Department of Anesthesia Techniques and Intensive Care, Al-Taff University College, Karbala, Iraq*

[4] *Department of Pharmaceutics, College of Pharmacy, Al-Zahraa University for Women, Karbala, Iraq*

[5] *Department of Pathobiology, Shahrekord Branch, Islamic Azad University, Shahrekord, Iran*

[6] *Student Research Committee, Shahrekord University of Medical Sciences, Shahrekord, Iran*

[7] *Department of Veterinary Surgery and Radiology, School of Veterinary Medicine, Shiraz University, Shiraz, Iran*

[8] *Department of Biology, Shahrekord Branch, Islamic Azad University, Shahrekord, Iran*

[9] *Department of Clinical Sciences, Faculty of Veterinary Medicine, Shahrekord University, Shahrekord, Iran*

[10] *Medical Plants Research Center, Basic Health Sciences Institute, Shahrekord University of Medical Sciences, Shahrekord, Iran*

ARTICLE INFO

Article History:
Received 27 January 2025
Accepted 25 March 2025
Published 01 April 2025

Keywords:
Chitosan
Platelet-rich plasma
Selenium nanoparticle
Transdermal drug delivery
Wound healing

ABSTRACT

The process of wound healing is complex and can be impaired by infection and inflammation. Chitosan (CS), selenium nanoparticles (SeNPs), and platelet-rich plasma (PRP) have individually shown promise in promoting wound healing due to their regenerative and antioxidant properties. However, their combined use in a transdermal patch for synergistic effects remains underexplored. This study aimed to develop and evaluate a novel chitosan-based transdermal patch incorporating SeNPs and PRP to explore their collective effectiveness in facilitating wound healing in a rat model. Seventy-five male Wistar rats with 1.5 × 1.5 cm^2 wounds were divided into five groups: control, free patch, CS/SeNPs, CS/PRP, and CS/SeNPs/PRP. Patches were prepared by dissolving chitosan in acetic acid, adding propylene glycol, SeNPs, and PRP, and then freeze-drying. Wound healing was assessed on days 3, 7, and 21 using histopathology, cytokine expression, and fluorescent immunohistochemistry for vascular growth factors. The CS/SeNPs/PRP patch significantly outperformed other treatment groups in terms of wound closure rate ($p < 0.05$). Histological analysis revealed enhanced re-epithelialization, collagen deposition, and angiogenesis. The observed reduction in inflammatory cytokine levels, specifically TNF-α and IL-6, suggests an anti-inflammatory effect contributing to the overall improvement in wound healing outcomes. This novel transdermal patch combining the beneficial properties of CS, SeNPs, and PRP offers a promising therapeutic approach for promoting wound healing through accelerated tissue regeneration and modulation of inflammation.

How to cite this article
Kaboli M., Hashim A., Altememy D. et al. Enhanced Wound Repair in Rats via a Chitosan-Based Transdermal Patch with Selenium Nanoparticles and Platelet-Rich Plasma. J Nanostruct, 2025; 15(2):771-787. DOI: 10.22052/JNS.2025.02.035

* *Corresponding Author Email: khosravian.p@skums.ac.ir*
javdani59@gmail.com

INTRODUCTION

The skin, a complex and multifunctional organ, acts as our body's outermost protective layer, constantly interacting with the external environment. It has a vital function in detecting stimuli, maintaining body temperature and shielding us from harm [1, 2]. Due to its exposure to the outdoor environment, the skin is highly susceptible to injury, making effective wound healing essential for restoring its anatomical integrity and functional status [2, 3].

Wounds are physical injuries that disrupt the skin's integrity and can be classified as chronic or acute [4]. Burns, surgical incisions and other traumatic injuries are acute wounds that recover quickly. A normal acute wound looks like a clean, non-infected surgery incisional wound that is closed with surgical sutures. Proper wound healing serves as essential for the recovery of interrupted anatomical integrity and functional status of the skin [3]. Proliferation, an inflammatory response and remodeling are the three parts of the complicated healing process framework that overlap frequently [5, 6]. The inflammatory phase includes cellular processes like the entry of leukocytes, which play distinct roles in killing microbes and making cytokines. This starts the cell proliferation response for wound repair and vascular reactions including blood clotting and stopping bleeding. During the proliferation phase, granulation tissue forms and the wound's surface becomes covered with cells. The subsequent remodeling phase focuses on restoring the skin's structural and functional integrity [7].

Several options are available for managing wound healing, including foam dressings, gauze, transparent film, hydrocolloid and hydrogel dressing, and transdermal patches [8]. Transdermal drug delivery systems (TDDS) are devices that administer drugs through the skin in a controlled and sustained manner, ensuring a consistent therapeutic effect [9].

Biopolymers that are derived from natural sources like plants, animals, or microbes, have found extensive applications in biomedicine due to their diverse properties and potential uses. Among these, chitosan, a biocompatible and biodegradable polymer derived from chitin (the main component of crustacean exoskeletons), has emerged as a valuable resource. Its safety, non-antigenicity, and biocompatibility make it suitable for various medical uses. The biodegradability of chitosan allows it to naturally break down within the body, while its hemostatic properties aid in blood clotting. Chitosan also boasts antimicrobial properties and accelerates healing by stimulating cell growth, blood vessel formation, and collagen production [10, 11]. Chitosan's adaptability makes it a strong contender for wound care applications. Other biomaterials like alginate and collagen have also shown potential in wound healing applications [12-15].

Selenium is one of the most crucial micronutrients for both humans and animals and is an essential trace element. Selenoproteins, a class of proteins containing the unique amino acid selenocysteine, have gotten an excessive amount of attention because of their diverse and interesting activities in biology. These proteins have essential functions in a range of physiological activities, including antioxidant defense, immune regulation and cellular signaling. Their anti-inflammatory activities aid in regulating immunological responses and their antioxidant abilities protect cells from oxidative damage. Additionally, selenoproteins have been shown to exhibit antimutagenic and anticarcinogenic activities, potentially playing a role in cancer prevention. Furthermore, these proteins possess antiviral, antibacterial and antifungal properties, contributing to the body's defense against infections. Selenium nanoparticles (SeNPs) are a promising alternative to elemental selenium due to their enhanced stability, biocompatibility and reduced toxicity [16, 17].

Recent research suggests that SeNPs combat bacteria and aid tissue repair. PRP, or platelet-rich plasma, is an extremely concentrated form of human plasma that contains an excessive amount of platelets within it and has also garnered attention for its role in promoting healing [18, 19]. Baseline platelet levels in plasma are usually 150,000/µl–350,000/µl. PRP is containing 1,000,000 platelets/µl in 5 ml of plasma. This concentration has been scientifically demonstrated to be effective in promoting healing in bones and soft tissues. Platelet-rich plasma (PRP) contains an abundance of growth factors such as platelet-derived growth factor (PDGF) which is crucial for cell proliferation, vascular endothelial growth factor (VEGF) which is essential for angiogenesis, transforming growth factor (TGF) which is involved in cell differentiation, and epidermal growth factor (EGF) which promotes cell growth and healing [20, 21]. Recent

research findings show that PRP can speed up the healing process [22-24]. In addition, chitosan, being a biopolymer, has proven notable efficacy in terms of its antimicrobial attributes and wound healing capabilities [25-27]. SeNPs possess ideal biomimetic characteristics of immune evasion and show remarkable antibiotic-free properties, giving them a promising candidate for clinical application in wound healing [28].

This study investigates the synergistic effects of incorporating chitosan, SeNPs and PRP into a TDDS for enhanced wound healing. The hypothesis is that this novel combination will accelerate wound closure, promote tissue regeneration and reduce inflammation compared to individual components or conventional treatments. By evaluating the efficacy of this combined approach in a rat model of acute wound healing, this study seeks to contribute to developing innovative and effective wound care therapies.

MATERIALS AND METHODS

Materials

Selenium dioxide powder, ascorbic acid, acetic acid, propylene glycol, and low molecular weight chitosan (50-190 kDa) were sourced from Sigma-Aldrich. BD Vacutainer ACD-A blood collection tubes (Vacutainer®, BD Biosciences) were used for blood collection, and phosphate-buffered saline tablets (Gibco™, Thermo Fisher Scientific) were used to prepare buffer solutions. All remaining chemicals were analytical grade.

Animals

Seventy-five male Wistar rats (180-250 g), sourced from the Pasteur Institute of Iran, were individually housed in standard plastic cages. These cages were maintained in a controlled environment with a consistent temperature and a 12-hour light-dark cycle, designed to simulate natural circadian rhythms. The rats were provided with unlimited access to both food and water throughout the duration of the study.

Preparation of SeNPs

Selenium nanoparticles (SeNPs) were synthesized through a reduction reaction. Selenium dioxide (55.5 mg) was dissolved in deionized water (500 ml), and ascorbic acid (387.2 mg) was dissolved in deionized water (50 ml). The latter solution was then slowly introduced into the former under vigorous stirring. The reduction reaction resulted in the formation of SeNPs, visually confirmed by a color change in the solution. After one hour of continuous stirring, SeNPs were collected by ultracentrifugation and washed multiple times with ethanol to remove impurities [29].

Nanoparticle characterization

Size, zeta potential and polydispersity index

The synthesized SeNPs were characterized by dynamic light scattering (DLS) for figuring out particle size, polydispersity index (PDI) and zeta potential. This analysis was performed using a Zetasizer Nano ZS instrument (Malvern Instruments, UK), which employs a 50 mW HeNe laser beam operating at a wavelength of 633 nm [30].

Morphology and elemental composition

After being placed on a glass surface and then allowed to air dry for a full day (24 hours), the SeNPs underwent gold-palladium sputter coating to enhance their conductivity and visibility under electron microscopy. Field emission scanning electron microscopy (FE-SEM, Tescan/Mira, Czech Republic) was employed to visualize the morphology of the SeNPs. The elemental composition of the SeNPs was determined using energy-dispersive X-ray spectroscopy (EDAX) in conjunction with field emission scanning electron microscopy (FE-SEM). This technique allowed for the verification of the presence of selenium within the nanoparticles and the generation of spectroscopic maps illustrating the elemental distribution of selenium [31].

PRP preparation

Blood (10 ml) was drawn from the heart of each rat into yellow tubes containing acid citrate dextrose (ACD) as an anticoagulant. The blood samples were centrifuged at 400 rpm for 10 minutes at 22 °C. Subsequently, a second centrifugation step was performed for an additional 10 minutes at 800 rpm to separate the platelet-rich plasma (PRP) from the platelet-poor plasma (PPP). Approximately 1.0 ml of PPP was collected as the supernatant, while approximately 0.5 ml of PRP was obtained from the bottom of the tube using a pipette [32].

Preparation of transdermal patch

The fabrication of the chitosan-based

transdermal patches involved a multi-step process. The initial step in preparing the transdermal patch involved, dissolving 100 mg of chitosan in 10 ml of a 1% acetic acid solution to create a uniform mixture. This process resulted in the formation of a homogenous mixture, ensuring uniform distribution of the chitosan throughout the solution. The acetic acid served as a solvent, facilitating the dissolution of chitosan and enabling its subsequent incorporation into the patch formulation. As a plasticizer, 0.2 ml of propylene glycol was subsequently incorporated into the patches to increase their flexibility and durability. Subsequently, 0.6 mg of selenium nanoparticles (SeNPs) and 30 µl of platelet-rich plasma (PRP) into the mixture. This combined solution was then carefully poured into 10 molds, each measuring 1×1 cm^2 were filled with one milliliter of the prepared solution, which was then freeze-dried and kept at 4 °C to prepare CS/SeNPs/PRP. On the other hand, Patches holding only SeNPs (CS/SeNPs) and PRP (CS/PRP) are synthesized in the same way [33-35].

Physicochemical evaluation

Appearance characterization

The prepared transdermal patches underwent visual inspection to evaluate their color, clarity, flexibility, homogeneity, and smoothness, ensuring uniformity, pliability, and the absence of air bubbles [36].

Swelling index study

After setting up the first weight (W_0) of the different patches, samples of the different TDDS formulas were put on a 2% agar plate and left to grow at 32 °C to find out their swelling index. At predetermined intervals, the patches were removed from the incubator, any extra water on their surface was removed using filter paper and the swelled patch was reweighed (W_t) [36, 37]. The swelling index was subsequently determined using the equation:

$$\text{Swelling index} = \frac{(Wt - W0)}{W0} \times 100 \quad (1)$$

By calculating the swelling index, researchers can gain insights into the patch's ability to absorb wound exudate, a critical factor in maintaining a moist wound environment and promoting healing.

Determination of surface pH

To assess the likelihood of mucosal irritation by the transdermal patches, the surface pH of TDDS with different formulations is measured. Skin irritation may result from an alkaline or acidic pH. Each patch sample received 5 ml of pH 7.4 phosphate buffer. The pH levels were then checked every 2, 4 and 6 hours by placing an electrode on the surface of the enlarged patch. It is considered that ideally, topical formulations should have a pH between 6 and 8 to avoid skin irritation [36].

In-vitro Bio-adhesive evaluation

There exist several in vitro methodologies for evaluating adhesion strength, which commonly rely on the measurement of the required force for detaching the patch from a level surface. The bio-adhesive strength of transdermal patches was assessed using a modified two-arm balance [36]. One arm of the balance was employed to suspend a beaker designed to collect water, while the other arm was used to suspend a glass surface that stuck to patches. To find the minimum adhesion force achievable between the patch and the mucus, a 2×2 cm^2 piece of rat skin was affixed to the base glass surface. Afterward, the designated patch was meticulously placed onto a small glass plate and kept near the corresponding cellulose membrane, which had been previously hydrated with distilled water. The water was then gradually added to the collecting vessel at a rate of 3 ml per minute. As soon as, the removing of the patch from the surface of the cellulose membrane, the water addition was halted and adhesion strength was found. The average result of this experiment was calculated after three replications [38].

In-vitro release of SeNPs

Release tests in vitro were conducted to assess the release pattern of SeNPs from the transdermal patch. Franz diffusion cells, a standard tool for evaluating drug release, were employed for this purpose. A 20 ml volume of phosphate buffer at pH 7.4 was added to each cell's receiver chamber to simulate physiological conditions. To simulate the skin barrier, a cellulose acetate membrane with a pore size of 0.45 µm was inserted between the donor (patch) and receiver chambers. The receiver chamber was kept at a consistent temperature of 37 °C using a heated magnetic stirrer and the solution was continuously agitated to achieve even dispersion of the released SeNPs. The samples

were gathered from the recipient compartment at regular times of 1, 2, 3, 4, 5, 6 and 8 hours. In order to maintain sink conditions, an equivalent volume of fresh phosphate buffer was introduced after each sampling. The SeNPs content in the collected samples was then quantified by employing UV-Vis spectrophotometry at a specific wavelength of 265 nm, which is where the SeNPs exhibit their greatest absorbance [39, 40].

In vivo wound healing study

For each surgical procedure, anesthesia was initiated through intraperitoneal administration of a combined ketamine (70 mg/kg) and xylazine

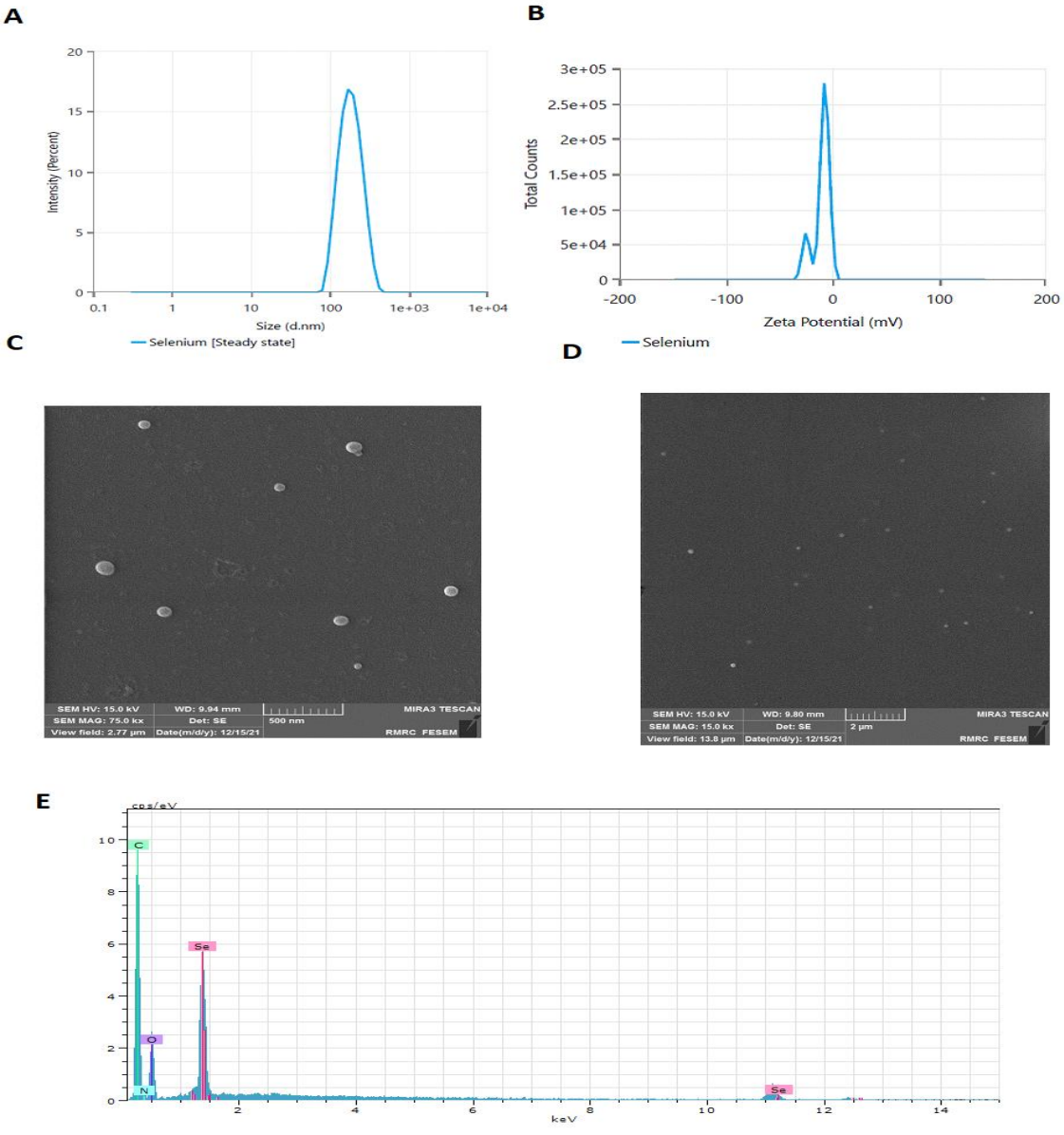

Fig. 1. SeNPs are described by: A) the size particle distribution, B) zeta potential of selenium nanoparticles (SeNPs) using Dynamic Light Scattering (DLS), C) FE-SEM image showing the morphology of SeNPs, D) SEM image of CS/SeNPs/PRP highlighting nanoparticle distribution and E) EDAX spectra confirming the presence of selenium in the nanoparticles.

(10 mg/kg) solution. After surgical preparation of the animal's dorsal skin, a square area measuring 1.5×1.5 cm^2 was excised using sterile scissors. Transdermal patches were promptly applied to the wounds, and the rats were placed in cages with limited numbers for individual monitoring and care, including wound assessment, dressing changes, and provision of food and water [40].

The rats were split into five groups at random (n=15 per group):

- Control group: No treatment
- Free patch group: Chitosan patch only
- CS/SeNPs group: Chitosan patch with selenium nanoparticles
- CS/PRP group: Chitosan patch with platelet-rich plasma
- CS/SeNPs/PRP group: Chitosan patch with both selenium nanoparticles and platelet-rich plasma

Gross observation of wound closure

To assess the progression healing of wounds, the size of each wound was measured on days 3, 7 and 21 after the surgical procedure. A digital caliper was used to obtain precise measurements of the wound dimensions and the wound area was subsequently calculated in square millimeters. This allowed for a quantitative assessment of wound closure over time in the different treatment groups [41, 42].

Histopathological examination

For histological analysis, skin samples from the wound site were carefully collected on days 3, 7 and 21 after the animal's demise, these samples included the dermis, epidermis and subcutaneous tissue. Following collection, skin samples from the wound site were fixed in a 4% formaldehyde solution and maintained at 4 °C to preserve tissue structure. Subsequently, the samples were dehydrated by using a series of ethanol solutions with increasing concentrations. Next, the dehydrated samples were embedded in paraffin wax, a process that provides structural support for sectioning. Thin sections were cut from the paraffin blocks and stained using standard histological techniques. The technique of hematoxylin and eosin (H&E) staining was utilized to examine the structure of the tissue as a whole, whereas Masson's trichrome staining was performed to specifically enhance the visibility of collagen fibers. The stained sections were subsequently analyzed using a light microscope (Axio Scope A1 FL; Carl Zeiss, Wetzlar, Germany) in order to evaluate the histological characteristics of the wound healing process [43, 44].

Statistical analysis

There were two parts to the statistical study of the experimental data. For non-parametric data, the Kruskal-Wallis's test. For parametric data, a one-way analysis of variance (ANOVA) was conducted, followed by Bonferroni post hoc tests. Results are presented as mean ± standard deviation (SD), with $p < 0.05$ considered statistically significant [45, 46].

RESULTS AND DISCUSSION

Zeta potential and particle size analysis of SeNPs

The SeNPs were characterized using DLS to figure out particle size distribution and zeta potential. The size distribution histogram had a shape that was very close to Gaussian, which means that the sizes were spread out fairly evenly. The polydispersity index (PDI) of 0.1731 indicated a narrow size distribution of the SeNPs. The zeta potential of the SeNPs was also found to be -10.07 mV (Fig. 1B). This negative zeta potential means that the SeNPs have a modest amount of electrostatic repulsion, which helps them stay in suspension and stops them from sticking together. These results are consistent with previous research on the synthesis and characterization of

Table 1. Surface pH of different patch formulations at regular time intervals, indicating their compatibility with skin contact and potential for irritation, shows the surface pH values of various transdermal patches measured at 2, 4 and 6-hour intervals. Data indicate the formulations' compatibility with skin contact, avoiding irritation.

	Time (hour)		
Patch formulation	2	4	6
CS/SeNPs	6.44 ± 0.44	6.59 ± 0.24	6.52 ± 0.31
CS/PRP	6.63 ± 0.21	6.71 ± 0.18	6.97 ± 0.75
CS/SeNPs/PRP	6.42 ± 0.37	6.77 ± 0.09	6.54 ± 0.26

All data are the mean ± SD of three independent experiments.

SeNPs, demonstrating the successful fabrication of stable and uniform nanoparticles suitable for incorporation into the transdermal patch.

Assessment of SeNPs morphological features via FE-SEM

To examine the morphology of the synthesized SeNPs, a measurement employing FESEM was carried out. The resulting FESEM image displayed a predominantly spherical shape of the SeNPs, which were seen to have a diameter of about 50 nm (Fig. 1C).

Evaluation of elemental composition of SeNPs by EDAX method

The EDAX technique is used to analyze component elements of samples. The fundamental principle underlying this method involves the excitation of the sample using X-ray radiation. The efficacy of this technique is attributed to the unique atomic structure of each element, resulting in the manifestation of a specific set of peaks on the electromagnetic emission spectra. In the context of SeNPs, EDAX analysis has shown the presence of selenium elements in the sample composition (Fig. 1E).

Physicochemical properties of prepared patches
Appearance characteristics

After the completion of the manufacturing process, a comprehensive visual inspection was carried out on the chitosan transdermal patch that had both PRP and SeNPs. Furthermore, the resulting patch showed a consistent, supple and smooth surface, devoid of any air bubbles. The color of the final product was seen to be red. Additionally, a scanning electron microscopy (SEM) image was obtained, which proved the homogeneity of nanoparticle distribution throughout the patch (Fig. 1D).

Surface pH

The potential for the transdermal patches to cause mucosal irritation was assessed by measuring their surface pH. Each patch sample was immersed in 5 ml of phosphate buffer solution, and precisely adjusted to a pH of 7.4, to accurately mimic the physiological pH conditions of the skin. The pH of the patch surface was then measured at regular intervals of 2, 4 and 6 hours using a pH meter (Table 1). The electrode of the pH meter was carefully placed on the surface of the swollen patch to obtain accurate readings. The findings of this analysis revealed that the pH values of the patches were within the range considered to be compatible with natural tissue. This suggests that the patches are unlikely to cause skin irritation upon application, as extreme pH values (either acidic or alkaline) can disrupt the skin's natural barrier and lead to irritation.

Swelling index

The swelling index investigations were conducted on the transdermal patch and the findings are presented in Table 2. The swelling studies proved a rise in the swelling index of the transdermal patch as time increased. According to the results obtained, the swelling index of chitosan hydrogels shows a notable range of 700% to 900%, thereby showing their remarkable capacity for water absorption.

In-vitro bio-adhesive

In the context of topical administration, the transdermal patch must show prolonged adhesion to the skin. Such an attribute would ease the enhancement of drug diffusion kinetics, thereby affording heightened bioavailability [47]. When the polymer is applied to the skin, it undergoes hydration, causing an interaction with the skin's mucous layer. Table 3 proves that bio-adhesive strength (1.68 g), the force of adhesion (0.0168 N) and detachment stress (168.33 N/m^2) of the CS/SeNPs patch are the lowest. Conversely, the CS/SeNPs/PRP patch shows the highest bio-adhesive strength (3.96 g), the force of adhesion (0.0396 N) and detachment stress (396.67 N/m^2). Based on the findings, it is reasonable to investigate the

Table 2. Swelling index of different patch formulations, highlighting their water absorption capabilities. The swelling index is a critical factor for drug release and wound dressing efficiency.

Patch formulation	W_0 (mg)	W_t (mg)	Swelling index (%)
CS/SeNPs	0.0076 ± 0.001	0.0749 ± 0.032	885.521 ± 12.335
CS/PRP	0.0072 ± 0.001	0.0686 ± 0.036	825.777 ± 9.032
CS/SeNPs/PRP	0.0088 ± 0.002	0.0739 ± 0.041	739.234 ± 14.941

All values represent the mean (± SD) of three separate experiments.

potential of SeNPs and PRP as an effective cross-linking agent that regulates excessive hydration and enhances mucoadhesive properties.

In-vitro Release of SeNPs

Fig. 2 illustrates the SeNPs release profile from CS/SeNPs transdermal patch in an in vitro setting. The evaluation revealed that the release of SeNPs from the patch followed a controlled pattern. Specifically, 39% of the nanoparticles were rapidly released within the first hour, while about 90% of the nanoparticles were released within 96 hours of the evaluation. These results show that the release of SeNPs from the CS/SeNPs patch is gradual and controlled.

In vivo experiment results

Wound size

Throughout the 21-day study period, the group treated with the CS/SeNPs/PRP patch consistently exhibited the smallest wound area compared to all other groups. Accordingly, the combination treatment resulted in a much faster rate of healing the wound. The CS/SeNPs/PRP patch significantly outperformed the control group in healing the wound, highlighting the therapeutic potential of

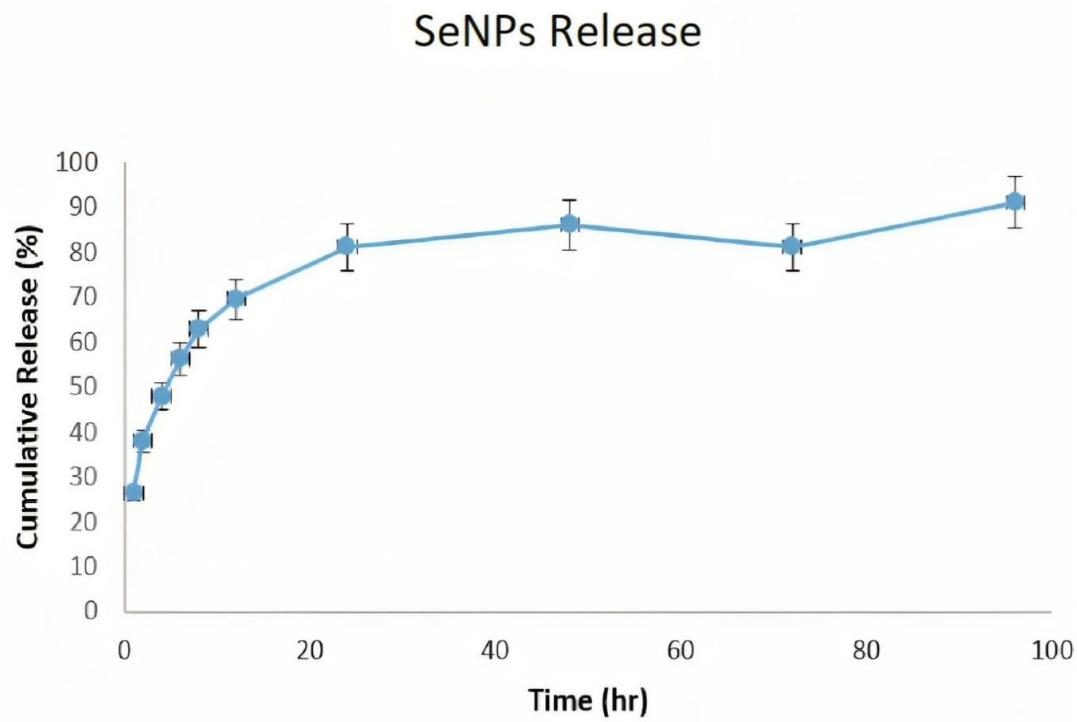

Fig. 2. In-vitro release profile of SeNPs from CS/SeNPs transdermal patch over 96 hours. The release pattern indicates a controlled and sustained release.

Table 3. In vitro bio-adhesion strength of different patch formulations, demonstrating their ability to maintain contact with the skin. This property is vital for effective drug delivery and wound treatment.

Patch formulation	Bio-adhesion time(s)	Bio-adhesive strength (g)	Force of adhesion (N)	Detachment stress (N/m^2)
CS/SeNPs	33.66 ± 2.49	1.68 ± 0.65	0.0168 ± 0.02	168.33 ± 4.33
CS/PRP	55.3 ± 6.5	2.76 ± 0.77	0.0276 ± 0.01	276.67 ± 6.81
CS/SeNPs/PRP	79.3 ± 2.62	3.96 ± 0.84	0.0396 ± 0.02	396.67 ± 7.58

All values represent the mean (± SD) of three separate experiments.

this novel patch formulation. While the CS/PRP and CS/SeNPs groups also demonstrated improved wound closure in comparison to the control, the CS/SeNPs/PRP group consistently outperformed them, suggesting a synergistic effect of the combined components (Fig. 3).

Histological observation of wound healing process

Investigation of the efficacy of various TDDS formulations, free patch, CS/SeNPs, CS/PRP and CS/SeNPs/PRP, in promoting wound healing, an analysis of histological changes in rat skin was conducted. The application of H&E staining revealed a gradual recovery and healing process of the inflicted injuries in all experimental groups. Notably, the CS/SeNPs/PRP group showed the most extensive restoration. On the third postoperative day, in all of the rats' wounds, a large amount of granulation tissue was seen. Nevertheless, the treated group with CS/SeNPs/PRP patch showed a greater presence of scar tissue compared to the other groups. Across all experimental groups, the regenerated dermis showed no signs of hair follicle or adnexal structure formation. Additionally, edema and inflammation were clear in the lesions of all groups (Fig. 4). On the seventh day, the process of re-epithelialization in wounds that were treated with CS/SeNPs/PRP commenced from the edges of the wound. Compared to the control group, the number of cells in the wound area dropped down after CS/SeNPs, CS/PRP and CS/SeNPs/PRP patches were administered, along with a more organized arrangement of collagen fibers and improved tissue alignment. The treated wounds also exhibited increased collagen density and lacked any signs of infection or edema (Fig. 5). On day 21, the wounds in the groups treated with the patch were fully closed, while the wounds in the control group showed incomplete epithelialization. In the CS/SeNPs and CS/SeNPs/PRP groups, the resulting scar tissue was smaller and the collagen fibers were better organized compared to the chitosan, CS/PRP and control groups. Furthermore, the treated groups demonstrated a decline in the number of mononuclear cells, particularly in the CS/SeNPs/PRP group and showed less edema and inflammation compared to the control group. Epidermal appendages, such as hair follicles, were absent in all experimental groups (Fig. 6). Additionally, the degree of inflammation and edema, collagen content, epithelialization, Neovascularization, hemorrhages and hyperemia were assessed histologically and categorized into four grades ranging from 0 to 3. Fig. 7, 8 and 9

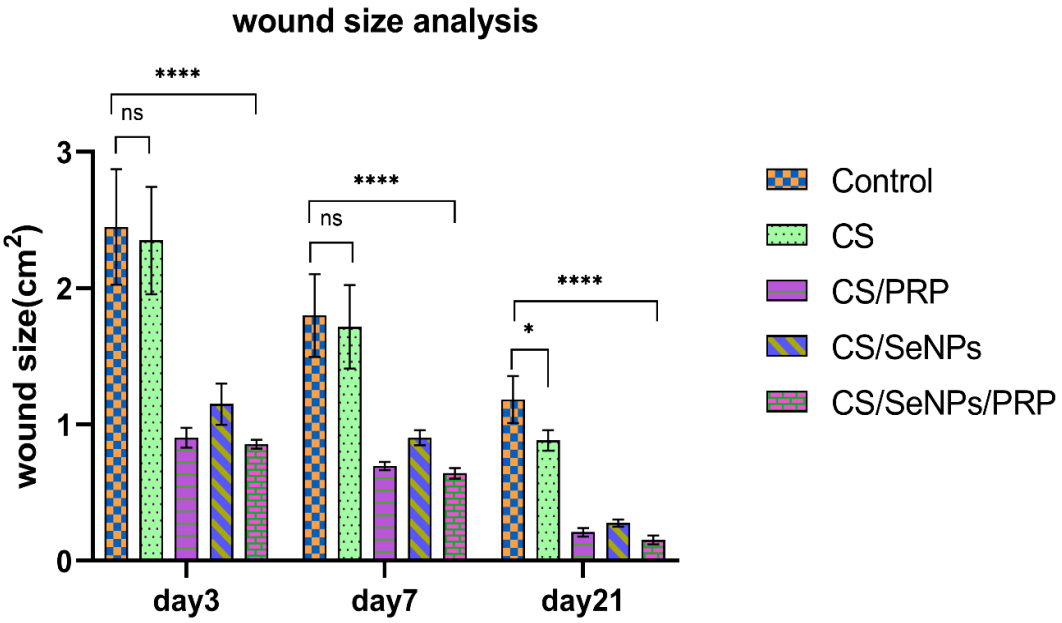

Fig. 3. Wound size reduction over time (days 3, 7 and 21) in different treatment groups. The data is displayed as the average value, with a sample size of 15. When compared to the control group, the difference is statistically significant ($p < 0.05$).

illustrate the alterations in the parameters on days 3, 7 and 21, respectively.

The wound is one of the most significant health system problems, affecting millions of people annually. The substantial economic burden of wound care in the United States is substantial, with millions of Medicare beneficiaries and tens of billions of dollars spent annually, highlighting

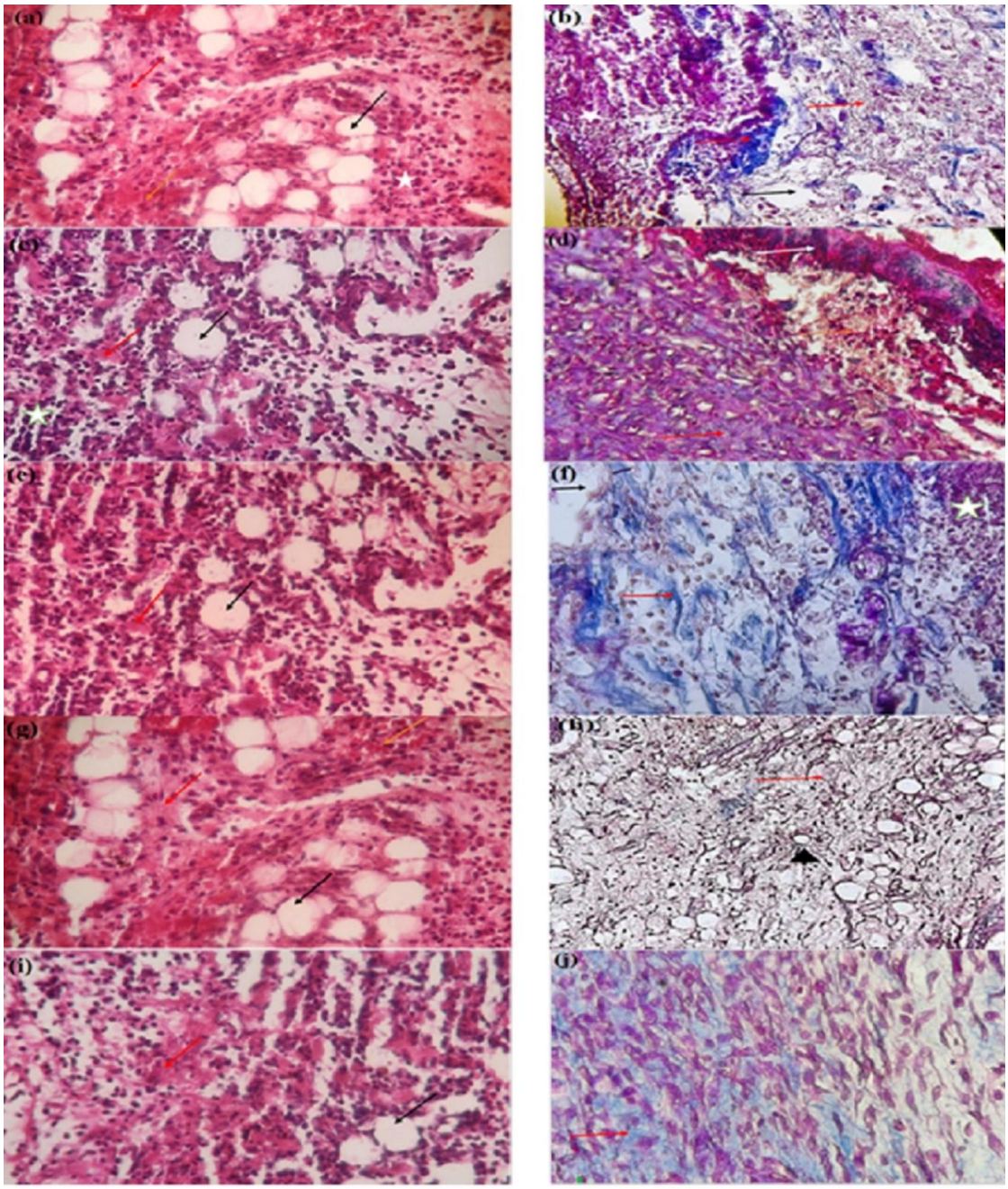

Fig. 4. Histological sections of rat wounds on day 3 post-treatment. Tissue samples were stained with H&E (a, c, e, g, i) and Masson's trichrome (b, d, f, h, j). Magnification: 400x. Black arrows indicate edema, red arrows indicate increased collagen deposition, white arrows indicate hemorrhage, white stars indicate edematous cells and black triangles indicate neovascularization.

the urgent need for innovative solutions [48, 49]. Unmanaged acute wounds can lead to complications like surgical site breakdown, pain, prolonged hospitalization, and increased morbidity, further emphasizing the importance of advancing wound care therapies [48-51].

This study investigated the combined effects of chitosan (CS), selenium nanoparticles (SeNPs), and platelet-rich plasma (PRP) in a transdermal patch to address this need. Chitosan, a biocompatible

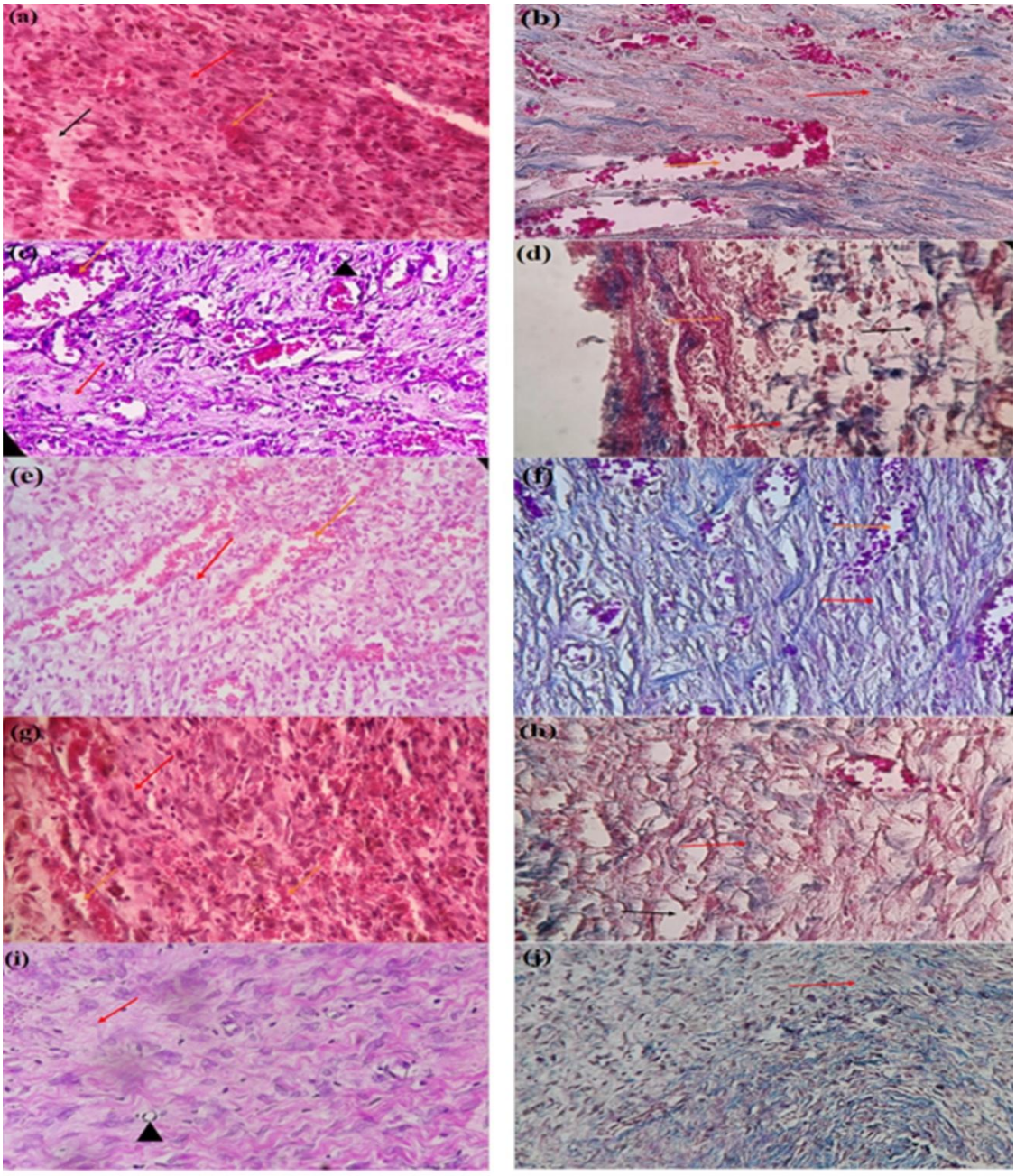

Fig. 5. Histological sections of rat wounds on day 7 post-treatment. Tissue samples were stained with H&E (a, c, e, g, i) and Masson's trichrome (b, d, f, h, j). Magnification: 400x. Black arrows indicate edema, red arrows indicate collagen synthesis, orange arrows indicate hemorrhage and black triangles indicate angiogenesis.

and biodegradable polymer, has emerged as a promising biomaterial for wound healing due to its regenerative properties [49]. Numerous studies have demonstrated the efficacy of chitosan-based formulations, PRP, and SeNPs in enhancing wound healing processes due to their regenerative, antimicrobial, and antioxidant properties. PRP, rich in growth factors, and SeNPs, with their antimicrobial and antioxidant properties, have also shown potential in wound healing. [52-57].

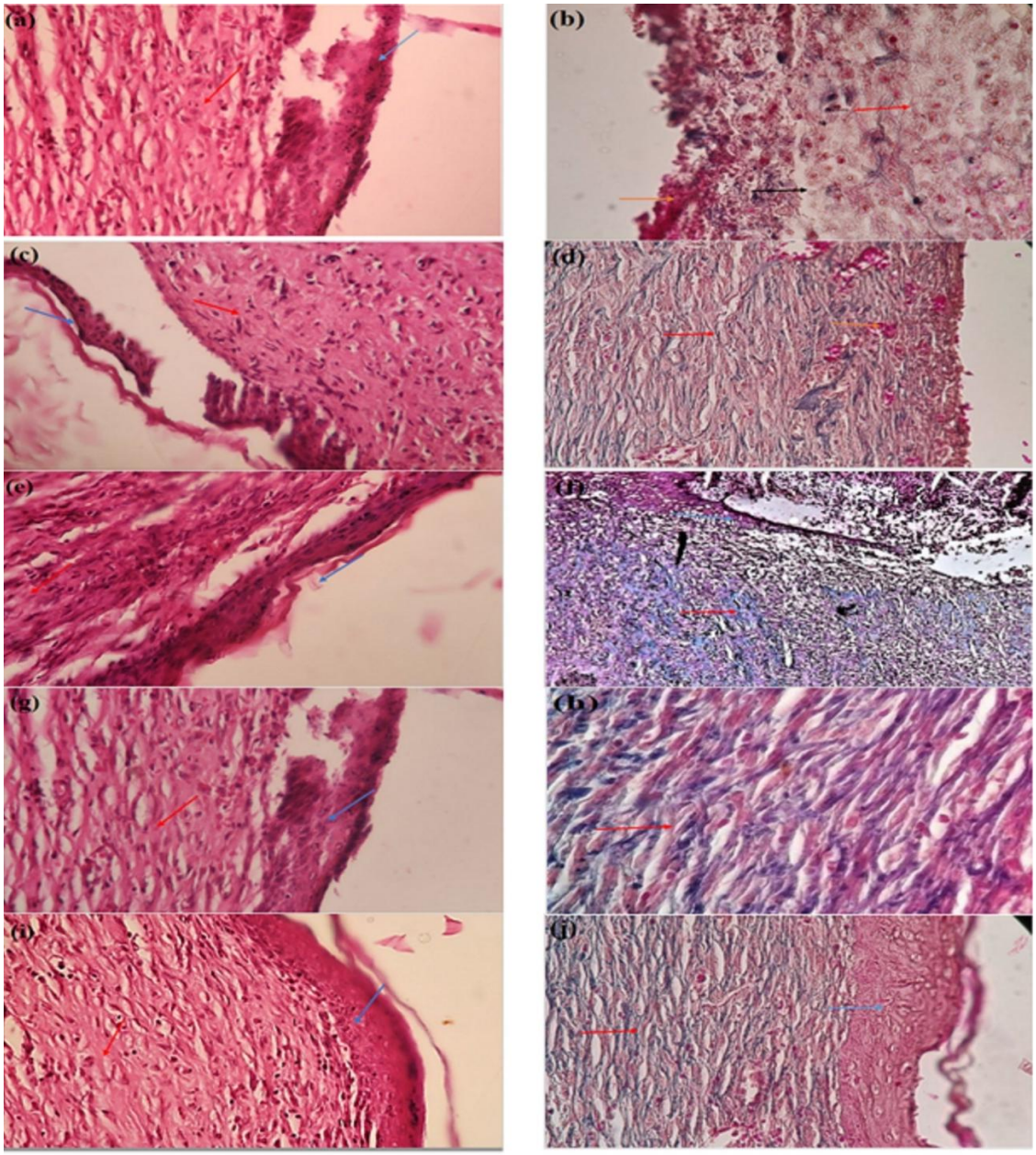

Fig. 6. Histological sections of rat wounds on day 21 post-treatment. Tissue samples were stained with H&E (a, c, e, g, i) and Masson's trichrome (b, d, f, h, j). Magnification: 400x. Black arrows indicate edema, red arrows indicate collagen fiber maturation, orange arrows indicate hemorrhage and blue arrows indicate epithelial layer formation.

This study's findings demonstrate the successful synthesis and characterization of SeNPs, revealing a spherical shape, uniform size distribution (average size 176.8 nm), and a negative zeta potential (-10.07 mV), indicative of good stability. The developed CS/SeNPs/PRP transdermal patch exhibited desirable characteristics for wound healing, including a suitable surface pH range (6.4 to 7). All formulations exhibited high moisture uptake, exudate-collecting capacity and bioadhesiveness, which are ideal characteristics for promoting wound healing. The transdermal patch having CS/SeNPs/PRP demonstrated a consistent, flexible and smooth surface, characterized by a uniform dispersion of SeNPs.

All formulations proved satisfactory bioadhesive properties, with CS/SeNPs/PRP exhibiting detachment stress 1.43 and 2.35 times higher than CS/PRP and CS/SeNPs, respectively. The swelling ratio of CS/SeNPs, CS/PRP and CS/SeNPs/PRP were 885.521, 825.777 and 739.234 respectively. The release of SeNPs from the chitosan matrix in the CS/SeNPs patch showed a controlled and sustained release with the non-burst pattern. EDAX analysis confirmed the presence of selenium in the SeNPs.

In vivo results demonstrated superior wound healing with the CS/SeNPs/PRP patch compared to other groups, evidenced by accelerated wound closure, which could be attributed to several mechanisms, enhanced re-epithelialization, collagen deposition, and angiogenesis. The patch also effectively reduced inflammatory cytokine levels (TNF-α, IL-6). The observed synergistic effects are likely due to the combined antioxidant, antimicrobial, and regenerative properties of the components. SeNPs protect cells from free radical damage, PRP stimulates tissue regeneration, and chitosan provides a conducive environment for healing. This can reduce inflammation and promote tissue regeneration. Additionally, SeNPs have been shown to have antimicrobial properties, which

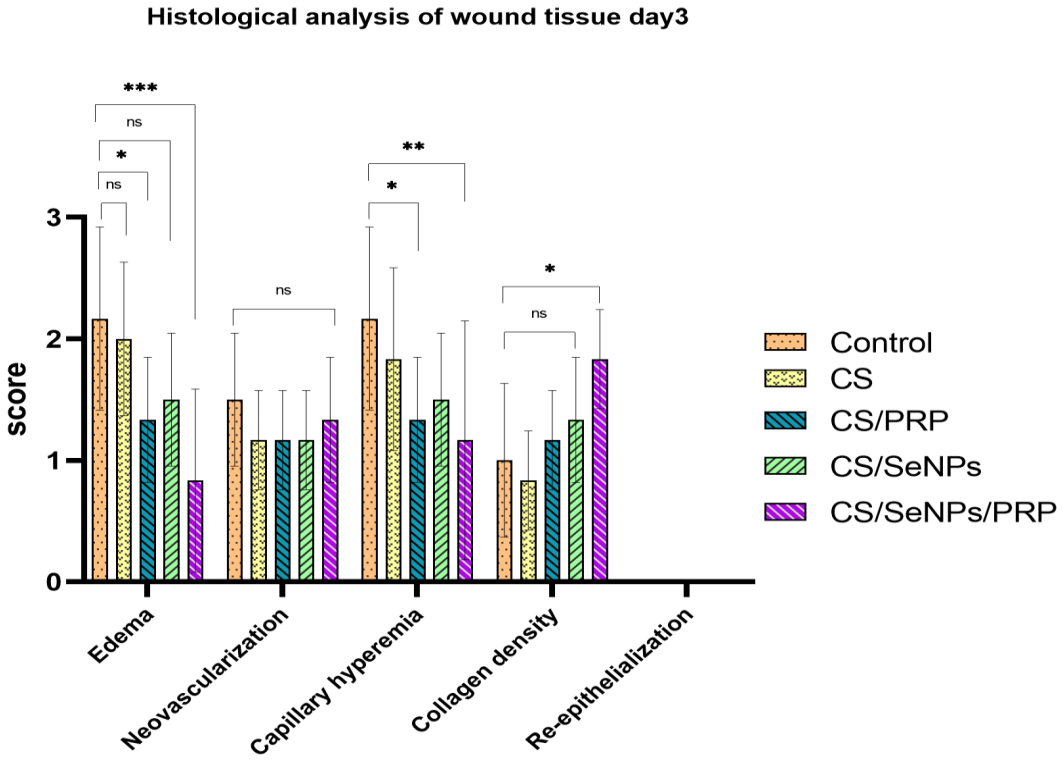

Fig. 7. Comparative histological scoring of wound healing parameters across different treatment groups on day 3, highlighting inflammation, collagen density and neovascularization.

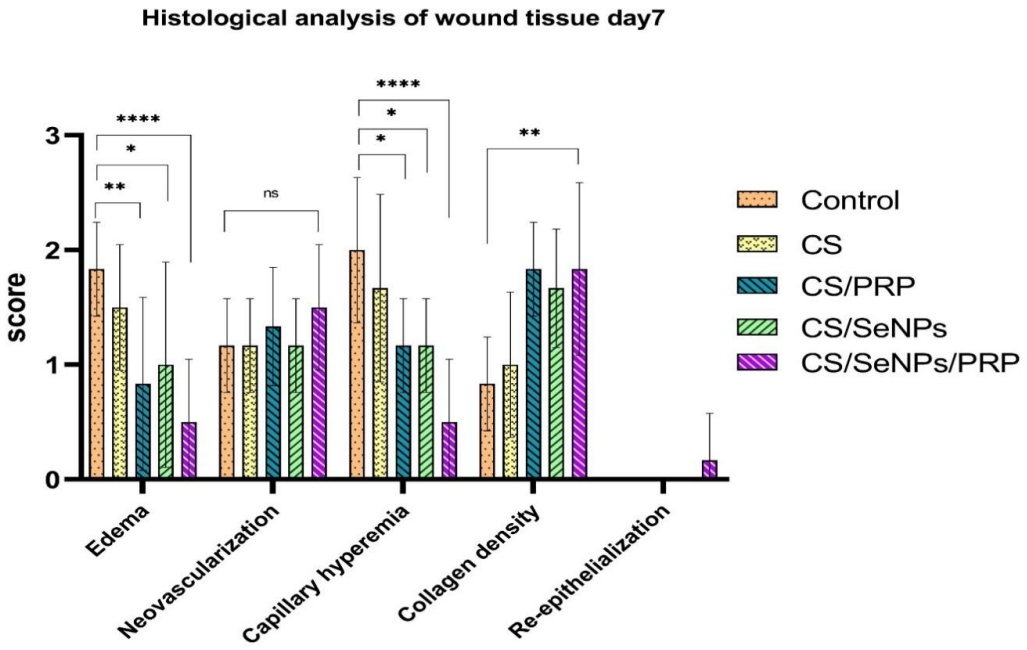

Fig. 8. Comparative histological scoring of wound healing parameters across different treatment groups on day 7, emphasizing the progress in tissue remodeling and epithelialization.

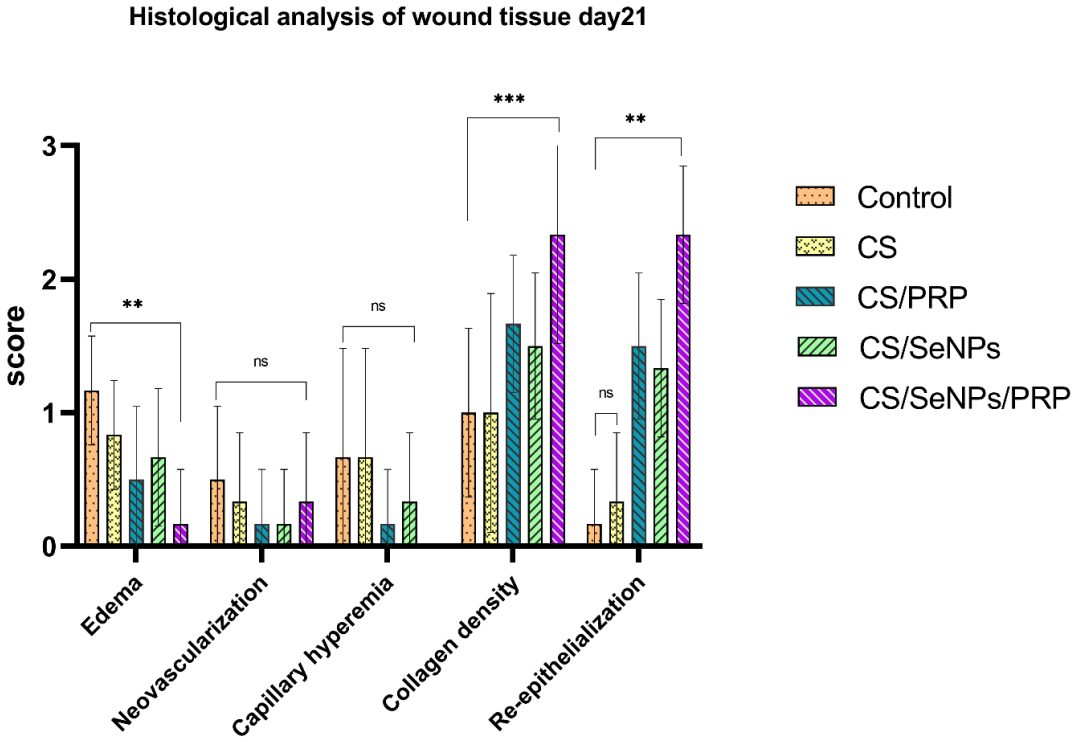

Fig. 9. Comparative histological scoring of wound healing parameters on day 21, illustrating final wound closure and tissue maturation among different treatment groups.

can help prevent infection and further damage to the wound site. PRP can stimulate cellular proliferation, promote angiogenesis, and enhance collagen synthesis, all of which are essential for wound healing. Furthermore, chitosan itself has been shown to have wound healing properties, such as promoting cell adhesion and migration, while also contributing to the maintenance of a moist microenvironment, that is conducive to healing. The incorporation of SeNPs and PRP into the chitosan patch may further enhance these properties, leading to accelerated wound closure and improved tissue regeneration observed in this study [58-61]. The CS/SeNPs/PRP patch offers a promising approach for promoting wound healing, for acute wounds, leveraging nanomedicine and regenerative medicine. This novel patch holds significant potential for benefiting patients with chronic wounds, which are notoriously challenging to heal and often carry a heightened risk of infection.

Additionally, the transdermal delivery system used in this study offers a convenient and non-invasive way to deliver therapeutic agents to the wound site. This could improve patient compliance and reduce the need for frequent dressing changes [62-64]. Transdermal drug delivery systems (TDDS) show promise as a substitute for oral administration and may potentially replace hypodermic injections [33, 65]. Further investigation is warranted to assess the long-term efficacy and safety of this particular patch, as well as to optimize its formulation for clinical applications in humans. Nonetheless, the results obtained in this study strongly suggest that the CS/SeNPs/PRP patch holds considerable potential as a safe and effective therapeutic intervention for diverse wound types.

CONCLUSION

Based on the information gathered for this study, it is possible to conclude that the CS/SeNPs/PRP patch is an appropriate framework for both the development and regeneration of skin cells, mostly due to its structure. SeNPs also play a key role in managing each step of wound healing. Platelet-rich plasma (PRP), abundant in growth factors, offers benefits for wound healing and tissue regeneration by acting as an anti-inflammatory agent, accelerating wound closure, and stimulating angiogenesis. Apparently, the combination of SeNPs and PRP in the chitosan scaffold can be a suitable method for treating and faster recovery of skin wounds as a control-release system.

ACKNOWLEDGMENT

The authors thank the Vice Chancellor for Research and Technology and the Phytochemical Laboratory staff for their support.

FUNDING

This research was funded by the Iran Government, By the Vice Chancellor for Research and Technology of Shahrekord University of Medical Sciences grant number 5943 and IR.SKUMS.REC.1401.040 ethical code in Shahrekord University of Medical Sciences.

CONFLICT OF INTEREST

The authors declare that there is no conflict of interests regarding the publication of this manuscript.

REFERENCES

1. Egawa G, Kabashima K. Barrier dysfunction in the skin allergy. Allergology International. 2018;67(1):3-11.
2. Nguyen AV, Soulika AM. The Dynamics of the Skin's Immune System. Int J Mol Sci. 2019;20(8):1811.
3. Chhabra S, Chhabra N, Kaur A, Gupta N. Wound Healing Concepts in Clinical Practice of OMFS. J Maxillofac Oral Surg. 2017;16(4):403-423.
4. Monaco JL, Lawrence WT. Acute wound healing. Clin Plast Surg. 2003;30(1):1-12.
5. Childs DR, Murthy AS. Overview of Wound Healing and Management. Surg Clin North Am. 2017;97(1):189-207.
6. Reinke JM, Sorg H. Wound Repair and Regeneration. Eur Surg Res. 2012;49(1):35-43.
7. Landén NX, Li D, Ståhle M. Transition from inflammation to proliferation: a critical step during wound healing. Cellular and molecular life sciences : CMLS. 2016;73(20):3861-3885.
8. Laurano R, Boffito M, Ciardelli G, Chiono V. Wound dressing products: A translational investigation from the bench to the market. Engineered Regeneration. 2022;3(2):182-200.
9. Jeong WY, Kwon M, Choi HE, Kim KS. Recent advances in transdermal drug delivery systems: a review. Biomaterials research. 2021;25(1):24-24.
10. Elangwe CN, Morozkina SN, Olekhnovich RO, Krasichkov A, Polyakova VO, Uspenskaya MV. A Review on Chitosan and Cellulose Hydrogels for Wound Dressings. Polymers. 2022;14(23):5163.
11. Alven S, Aderibigbe BA. Chitosan and Cellulose-Based Hydrogels for Wound Management. Int J Mol Sci. 2020;21(24):9656.
12. Boateng JS, Matthews KH, Stevens HNE, Eccleston GM. Wound Healing Dressings and Drug Delivery Systems: A Review. J Pharm Sci. 2008;97(8):2892-2923.
13. Lee KY, Mooney DJ. Alginate: properties and biomedical applications. Prog Polym Sci. 2012;37(1):106-126.
14. Chattopadhyay S, Raines RT. Review collagen-

based biomaterials for wound healing. Biopolymers. 2014;101(8):821-833.
15. Prasathkumar M, Sadhasivam S. Chitosan/Hyaluronic acid/ Alginate and an assorted polymers loaded with honey, plant, and marine compounds for progressive wound healing—Know-how. Int J Biol Macromol. 2021;186:656-685.
16. Skalickova S, Milosavljevic V, Cihalova K, Horky P, Richtera L, Adam V. Selenium nanoparticles as a nutritional supplement. Nutrition. 2017;33:83-90.
17. Hariharan S, Dharmaraj S. Selenium and selenoproteins: it's role in regulation of inflammation. Inflammopharmacology. 2020;28(3):667-695.
18. Cao J, Zhang Y, Zhang P, Zhang Z, Zhang B, Feng Y, et al. Turning gray selenium into a nanoaccelerator of tissue regeneration by PEG modification. Bioactive materials. 2022;15:131-144.
19. Ahmed MK, Moydeen AM, Ismail AM, El-Naggar ME, Menazea AA, El-Newehy MH. Wound dressing properties of functionalized environmentally biopolymer loaded with selenium nanoparticles. J Mol Struct. 2021;1225:129138.
20. Marx RE. Platelet-Rich Plasma (PRP): What Is PRP and What Is Not PRP? Implant Dent. 2001;10(4):225-228.
21. Wei S, Xu P, Yao Z, Cui X, Lei X, Li L, et al. A composite hydrogel with co-delivery of antimicrobial peptides and platelet-rich plasma to enhance healing of infected wounds in diabetes. Acta Biomater. 2021;124:205-218.
22. Long DW, Johnson NR, Jeffries EM, Hara H, Wang Y. Controlled delivery of platelet-derived proteins enhances porcine wound healing. Journal of controlled release : official journal of the Controlled Release Society. 2017;253:73-81.
23. Zhao M, Wang J, Zhang J, Huang J, Luo L, Yang Y, et al. Functionalizing multi-component bioink with platelet-rich plasma for customized in-situ bilayer bioprinting for wound healing. Materials today Bio. 2022;16:100334-100334.
24. Xu K, Deng S, Zhu Y, Yang W, Chen W, Huang L, et al. Platelet Rich Plasma Loaded Multifunctional Hydrogel Accelerates Diabetic Wound Healing via Regulating the Continuously Abnormal Microenvironments. Advanced Healthcare Materials. 2023;12(28).
25. Dai T, Tanaka M, Huang Y-Y, Hamblin MR. Chitosan preparations for wounds and burns: antimicrobial and wound-healing effects. Expert Rev Anti Infect Ther. 2011;9(7):857-879.
26. R N, M K, J P, K.S V, Arpana C, Balashanmugam P, et al. Enhanced wound healing by PVA/Chitosan/Curcumin patches: In vitro and in vivo study. Colloids Surf B Biointerfaces. 2019;182:110339.
27. Kalalinia F, Taherzadeh Z, Jirofti N, Amiri N, Foroghinia N, Beheshti M, et al. Evaluation of wound healing efficiency of vancomycin-loaded electrospun chitosan/poly ethylene oxide nanofibers in full thickness wound model of rat. Int J Biol Macromol. 2021;177:100-110.
28. Fang M, Zhang H, Wang Y, Zhang H, Zhang D, Xu P. Biomimetic selenium nanosystems for infectious wound healing. Engineered Regeneration. 2023;4(2):152-160.
29. Mazarei M, Mohammadi Arvejeh P, Mozafari MR, Khosravian P, Ghasemi S. Anticancer Potential of Temozolomide-Loaded Eudragit-Chitosan Coated Selenium Nanoparticles: In Vitro Evaluation of Cytotoxicity, Apoptosis and Gene Regulation. Nanomaterials (Basel, Switzerland). 2021;11(7):1704.
30. Yan F, Li H, Zhong Z, Zhou M, Lin Y, Tang C, et al. Co-Delivery of Prednisolone and Curcumin in Human Serum Albumin Nanoparticles for Effective Treatment of Rheumatoid Arthritis. International journal of nanomedicine. 2019;14:9113-9125.
31. Yilmaz MT, İspirli H, Taylan O, Dertli E. A green nano-biosynthesis of selenium nanoparticles with Tarragon extract: Structural, thermal, and antimicrobial characterization. LWT. 2021;141:110969.
32. Carvalho A, Ferreira AF, Soares M, Santos S, Tomé P, Machado-Simões J, et al. Optimization of Platelet-Rich Plasma Preparation for Regenerative Medicine: Comparison of Different Anticoagulants and Resuspension Media. Bioengineering (Basel, Switzerland). 2024;11(3):209.
33. Loo HL, Goh BH, Lee L-H, Chuah LH. Application of chitosan-based nanoparticles in skin wound healing. Asian journal of pharmaceutical sciences. 2022;17(3):299-332.
34. Kaur M, Sharma A, Puri V, Aggarwal G, Maman P, Huanbutta K, et al. Chitosan-Based Polymer Blends for Drug Delivery Systems. Polymers. 2023;15(9):2028.
35. Altememy D, Javdani M, Khosravian P, Khosravi A, Moghtadaei Khorasgani E. Preparation of Transdermal Patch Containing Selenium Nanoparticles Loaded with Doxycycline and Evaluation of Skin Wound Healing in a Rat Model. Pharmaceuticals (Basel). 2022;15(11):1381.
36. Amorós-Galicia L, Nardi-Ricart A, Verdugo-González C, Arroyo-García CM, García-Montoya E, Pérez-Lozano P, et al. Development of a Standardized Method for Measuring Bioadhesion and Mucoadhesion That Is Applicable to Various Pharmaceutical Dosage Forms. Pharmaceutics. 2022;14(10):1995.
37. Menazea AA, Abdelbadie SA, Ahmed MK. Manipulation of AgNPs coated on selenium/carbonated hydroxyapatite/ ε-polycaprolactone nano-fibrous via pulsed laser deposition for wound healing applications. Appl Surf Sci. 2020;508:145299.
38. Schlund M, Dartus J, Defrançois S, Ferri J, Delattre J, Blanchemain N, et al. In Vitro and In Vivo Evaluation of a Bio-Inspired Adhesive for Bone Fixation. Pharmaceutics. 2023;15(4):1233.
39. Shahabadi N, Zendehcheshm S, Khademi F. Selenium nanoparticles: Synthesis, in-vitro cytotoxicity, antioxidant activity and interaction studies with ct-DNA and HSA, HHb and Cyt c serum proteins. Biotechnology reports (Amsterdam, Netherlands). 2021;30:e00615-e00615.
40. Azis HA, Taher M, Ahmed AS, Sulaiman WMAW, Susanti D, Chowdhury SR, et al. In vitro and In vivo wound healing studies of methanolic fraction of Centella asiatica extract. S Afr J Bot. 2017;108:163-174.
41. Morton LM, Phillips TJ. Wound healing and treating wounds. J Am Acad Dermatol. 2016;74(4):589-605.
42. Turk M, Biernaskie J, Mahoney DJ, Jenne CN. Intravital Microscopy Techniques to Image Wound Healing in Mouse Skin. Methods in Molecular Biology: Springer US; 2022. p. 165-180.
43. Fischer AH, Jacobson KA, Rose J, Zeller R. Hematoxylin and Eosin Staining of Tissue and Cell Sections. Cold Spring Harbor Protocols. 2008;2008(5):pdb.prot4986.
44. Ozawa H. Principles and basics of immunohistochemistry. Folia Pharmacologica Japonica. 2019;154(4):156-164.
45. Armstrong RA. When to use the B onferroni correction. Ophthalmic Physiol Opt. 2014;34(5):502-508.
46. Lee SW. Methods for testing statistical differences between groups in medical research: statistical standard and

guideline of Life Cycle Committee. Life Cycle. 2022;2.
47. Rahman L, Lembang RS, Lallo S, Handayani SR, Usmanengsi, Permana AD. Bioadhesive dermal patch as promising approach for improved antibacterial activity of bioactive compound of Zingiber cassumunar Roxb in ex vivo Staphylococcus aureus skin infection model. J Drug Deliv Sci Technol. 2021;63:102522.
48. Ruiz PBdO, Lima AFC. Average direct costs of outpatient, hospital, and home care provided to patients with chronic wounds. Revista da Escola de Enfermagem da U S P. 2022;56:e20220295-e20220295.
49. Baharlouei P, Rahman A. Chitin and Chitosan: Prospective Biomedical Applications in Drug Delivery, Cancer Treatment, and Wound Healing. Mar Drugs. 2022;20(7):460.
50. Sen CK. Human Wounds and Its Burden: An Updated Compendium of Estimates. Adv Wound Care. 2019;8(2):39-48.
51. ACUTE WOUNDS. Wound Healing: CRC Press; 2005. p. 31-34.
52. Rasool A, Ata S, Islam A. Stimuli responsive biopolymer (chitosan) based blend hydrogels for wound healing application. Carbohydr Polym. 2019;203:423-429.
53. Bagher Z, Ehterami A, Safdel MH, Khastar H, Semiari H, Asefnejad A, et al. Wound healing with alginate/chitosan hydrogel containing hesperidin in rat model. J Drug Deliv Sci Technol. 2020;55:101379.
54. Nooshabadi VT, Khanmohamadi M, Valipour E, Mahdipour S, Salati A, Malekshahi ZV, et al. Impact of exosome-loaded chitosan hydrogel in wound repair and layered dermal reconstitution in mice animal model. Journal of Biomedical Materials Research Part A. 2020;108(11):2138-2149.
55. Ni X, Shan X, Xu L, Yu W, Zhang M, Lei C, et al. Adipose-derived stem cells combined with platelet-rich plasma enhance wound healing in a rat model of full-thickness skin defects. Stem Cell Res Ther. 2021;12(1):226-226.
56. Qian Z, Wang H, Bai Y, Wang Y, Tao L, Wei Y, et al. Improving Chronic Diabetic Wound Healing through an Injectable and Self-Healing Hydrogel with Platelet-Rich Plasma Release. ACS Applied Materials & Interfaces. 2020;12(50):55659-55674.
57. Golmohammadi R, Najar-Peerayeh S, Tohidi Moghadam T, Hosseini SMJ. Synergistic Antibacterial Activity and Wound Healing Properties of Selenium-Chitosan-Mupirocin Nanohybrid System: An in Vivo Study on Rat Diabetic Staphylococcus aureus Wound Infection Model. Sci Rep. 2020;10(1):2854-2854.
58. Singh R, Lillard JW, Jr. Nanoparticle-based targeted drug delivery. Exp Mol Pathol. 2009;86(3):215-223.
59. Rajinikanth B S, Rajkumar DSR, K K, Vijayaragavan V. Chitosan-Based Biomaterial in Wound Healing: A Review. Cureus. 2024;16(2):e55193-e55193.
60. Rai M, Ingle AP, Gupta I, Brandelli A. Bioactivity of noble metal nanoparticles decorated with biopolymers and their application in drug delivery. Int J Pharm. 2015;496(2):159-172.
61. Dhillon RS, Schwarz EM, Maloney MD. Platelet-rich plasma therapy - future or trend? Arthritis research & therapy. 2012;14(4):219-219.
62. Dhivya S, Padma VV, Santhini E. Wound dressings - a review. Biomedicine. 2015;5(4):22-22.
63. Moura LIF, Dias AMA, Carvalho E, de Sousa HC. Recent advances on the development of wound dressings for diabetic foot ulcer treatment—A review. Acta Biomater. 2013;9(7):7093-7114.
64. Nandhini J, Karthikeyan E, Rajeshkumar S. Nanomaterials for wound healing: Current status and futuristic frontier. Biomedical Technology. 2024;6:26-45.
65. Prausnitz MR, Langer R. Transdermal drug delivery. Nat Biotechnol. 2008;26(11):1261-1268.